New templates for the analysis of Aromatic Infrared Bands in the JWST era

Sacha Foschino[1], Olivier Berné[1], Christine Joblin[1]

Email: sacha.foschino@irap.omp.eu
[1]IRAP, Université de Toulouse, CNRS, CNES, UPS, (Toulouse), France

1/ Abstract

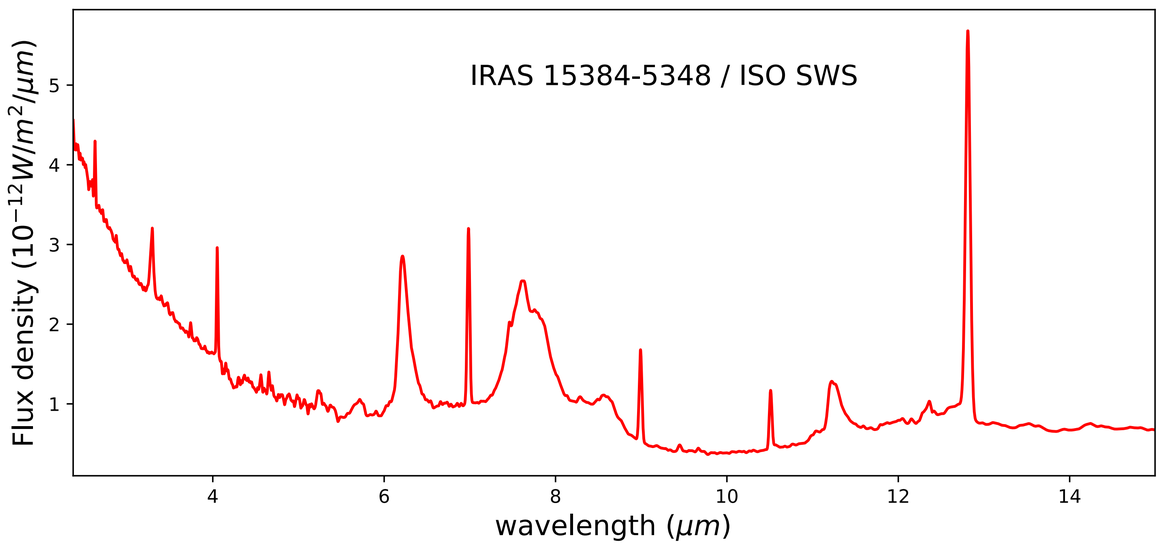

Fig. 1. ISO-SWS Mid-IR spectrum of IRAS 15384-5348 from [5].

Observations of the mid-infrared (mid-IR, 3-15μm, Fig. 1) spectra of photo-dissociation regions (PDRs) reveals ubiquitous and intense emission bands, at 3.3, 6.2, 7.7, 11.2 and 12.7 μm, called Aromatic Infrared Bands (AIBs) and attributed to polycyclic aromatic hydrocarbons (PAHs) [1]. The application of a blind signal separation (BSS) algorithm, i.e. the non-negative matrix factorization (NMF) of Lee & Seung [2] to a sample of Spitzer-IRS data was earlier used to extract at least three spectra in reflection nebulae (RNe). These were attributed to cationic and neutral PAHs (resp. PAH^+ and PAH^0) and evaporating very small grains (eVSG) [3]. A fourth component attributed to large, ionized PAH (PAHx) was invoked to better fit the spectra of planetary nebulae (PNe) [4].

We developed an approach to extract elementary spectra from archival ISO-SWS data [5]. These data have higher spectral resolution ($R \sim 260$ instead of $R \sim 70$) over a larger spectral range (here 2.3 to 15 μm instead of 5.5 to 14μm), but with no spatial information. We compensate this limitation by using the spectrum from different astrophysical objects. This work is done in preparation for the launch of the JWST in 2018.

2/ Modeling the data

As fig.1 shows, a typical mid-IR spectrum is composed of four main parts: gas lines (very narrow features), AIBs from PAHs and very small grains (broad features), a continuum carried by large and in thermal equilibrium grains and the instrumental noise. The data are considered to be a linear sum of all these contributions. In this study, all but the AIBs will be considered as noise and removed from the data.

$$\begin{cases} I_\lambda^{obs} = I_\lambda^{AIBs} + N_\lambda \\ N_\lambda = n_\lambda^{cont} + n_\lambda^{gas} + n_\lambda^{inst} \end{cases}$$

To subtract N from the data (I_λ^{obs}) and obtain as estimate of I_λ^{AIBs} ($\widehat{I}_\lambda^{AIBs}$) we chose to fit them with a L1-regularized non-negative least square algorithm using a catalog of blackbodies to fit the continuum and gaussians to fit the gas lines and AIBs.
Then we apply BSS on $\widehat{I}_\lambda^{AIBs}$.

3/ Blind Signal Separation

We assume that our n AIBs spectra of m points $\widehat{I}_\lambda^{AIBs}$ are a linear combination of a set of r elementary spectra whose the variation of the contributions implies the spectral variations from one spectrum to another. This gives the following model:

$$\widehat{I}_\lambda^{AIBs} = A \times S \begin{cases} \widehat{I}_\lambda^{AIBs} : AIB\ matrix,\ (n \times m) \\ A : weight\ matrix,\ (n \times r) \\ S : elementary\ spectra,\ (r \times m) \end{cases}$$

Lin (2007) [6] algorithm of non-negative matrix factorization (NMF) allows us to estimate A and S by respectively $\hat{A}$ and $\hat{S}$.
We initialized the algorithm with a new geometrical method of BSS, the Maximum Angle Signal Separation (MASS, [7]).

4/ Results of the extraction

Here, we applied NMF to $\widehat{I}_\lambda^{AIBs}$ with $n = 31$ spectra of $m = 7949$ points and chose to extract $r = 4$ elementary spectra using the same methodology proposed in Berné et al. 2007 [3]. Fig. 2 shows the result normalized at the maximum compared to the templates obtained from [3] and [4] by Pilleri et al. (2012) [10].

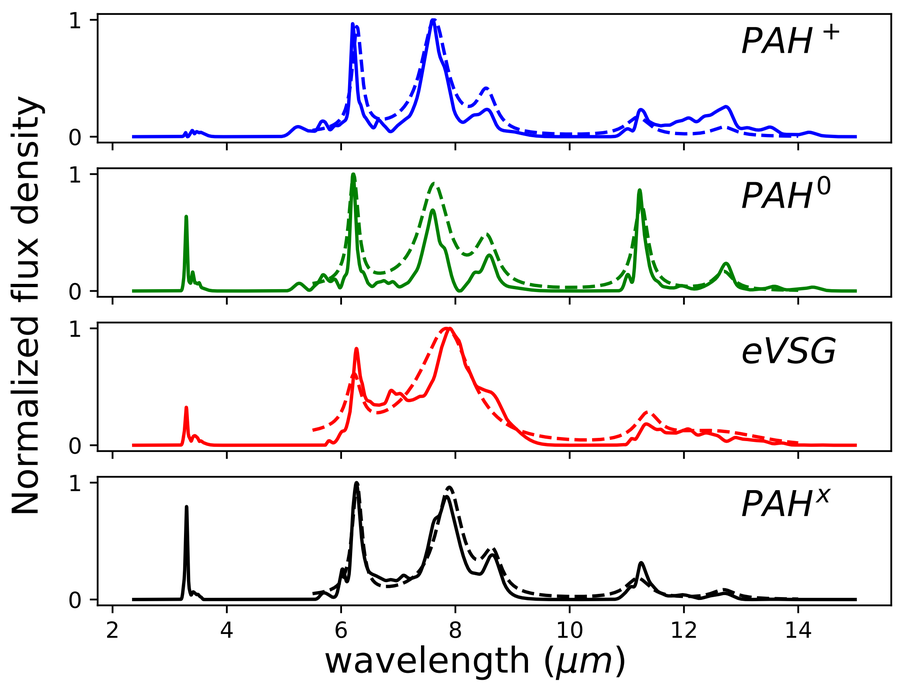

Fig. 2. Elementary spectra, lines of $\hat{S}$ (solid lines) and templates from [8] (dashed lines) normalized.

- 4 elementary spectra were extracted over a larger spectral domain than former studies with a higher spectral resolution of $R \sim 260$.
- Three out of four correspond to the already attributed families cationic and neutral PAHs resp. in blue and green in Fig. 2 and eVSGs in red.
- A fourth elementary spectrum has been extracted which corresponds to large and ionized PAHs, PAH^x in black, fig. 2. It's the first extraction of this spectrum with a BSS method.
- All of them are in good agreement with those of [8] and show more details over a larger spectral domain.

5/ Application

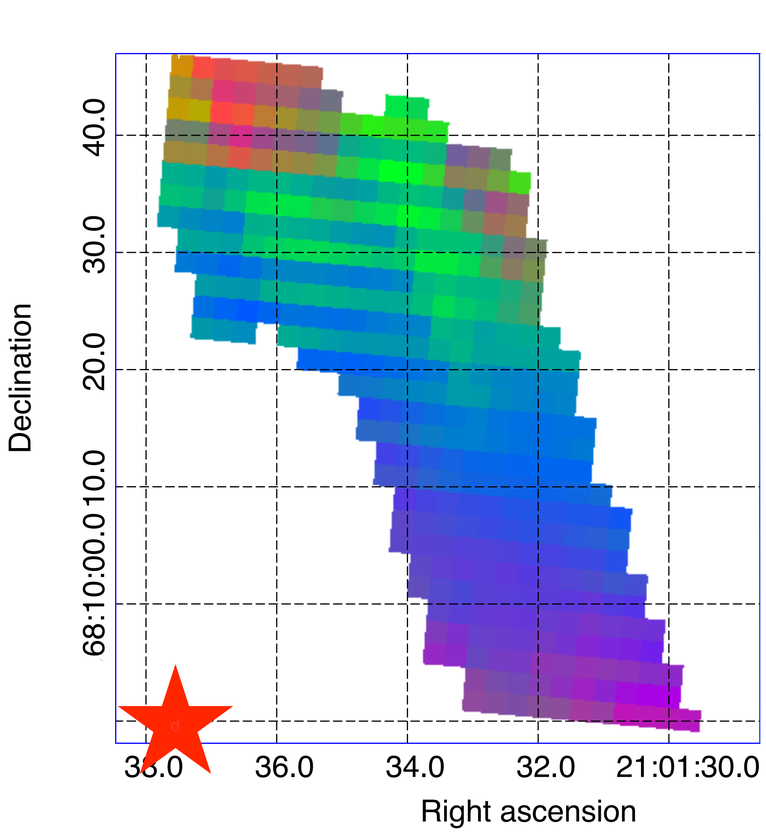

Fig. 3. Emission distribution of elementary spectra (without PAH^x) in the PDR NGC 7023 NW.

Using these four elementary spectra as a basis to fit mid-IR spectra, one can obtain the proportion of each population in the spectrum. When spatial information is available, as hyperspectral cube can provide, one can fit each spectrum of the cube and map the emission of each population in a same astrophysical object.

We used Akari IRC [9] and Spitzer IRS hyperspectral cubes of the PDR at the north west of NGC 7023 (which have complementary spectral range) that we have merged to get one hyperspectral cube from 2.5 to 15 μm with a spectral resolution of $R \sim 70$ of the same region.

Fig. 3 shows the map of the emission of eVSGs (red), PAH^0 (green) and PAH^+ (blue). The red star shows the position of the star HD 200775 which irradiates its surrounding cloud.
This distribution map of the differents elementary spectra is consistent with that of [3] and shows the chemical evolution of PAHs and eVSGs in an irradiated medium. It confirms the consistence of the extraction

References

[1] Leger, A. and Puget, J.L., A&A, 137, L5-L8, 1984
[2] Lee, D. D. and Seung, H.S., Advances in neural information processing systems, 556-562, 2001.
[3] Berné, O. et al., A&A, 469, 575-586, 2007.
[4] Joblin, C. et al., A&A, 490, 189-196, 2008.
[5] Peeters, E. et al., A&A, 390, 1089-1113, 2002.
[6] C.-J. Lin. Neural Computation, 19(2007), 2756-2779.
[7] A. Boulais et al., IEEE ECMSM, 2015, 1-6
[8] P. Pilleri et al., A&A, 2012, 545, A69
[9] P. Pilleri et al., A&A, 2015, 577, A16